

Impact of Alzheimer's Disease on the Functional Connectivity of Spontaneous Brain Activity

Christian Sorg^{1,*}, Valentin Riedl², Robert Perneczky¹, Alexander Kurz¹ and Afra M. Wohlschläger³

¹Department of Psychiatry, Klinikum rechts der Isar, Technische Universität München, Ismaninger Strasse 22, 81675 Munich, Germany; ²Department of Neurology, Klinikum rechts der Isar, Technische Universität München, Ismaninger Strasse 22, 81675 Munich, Germany; ³Department of Neuroradiology, Klinikum rechts der Isar, Technische Universität München, Ismaninger Strasse 22, 81675 Munich, Germany

Abstract: Alzheimer's disease (AD) prominently affects the structure and function of cerebral networks. Reflecting the complex network structure of the brain, spontaneous brain activity is organized by synchronized activity across distinct temporal and spatial scales. Temporal correlations of the functional MRI (fMRI) signal during rest have been used to characterize the impact of AD on the functional connectivity of spontaneous brain activity. Here we review studies using resting-state fMRI (rs-fMRI) to explore AD-induced changes of synchronized intrinsic activity at three levels of brain organization: the regional, inter-regional and large-scale level. Changes in posterior areas of the default network (DN) and the medial temporal lobes seem to be central to AD. These areas show remarkable disturbances in neuronal communication at all spatial levels and in very early stages of the disease. Finally, rs-fMRI seems to have the potential to produce connectivity-related biomarkers that distinguish AD and healthy aging.

Keywords: Alzheimer's disease, spontaneous brain activity, functional connectivity, fMRI, resting state, resting state networks, small world, local integration.

INTRODUCTION

Alzheimer's disease (AD) is the most prevalent cause of dementia in older adults [1]. AD-related dementia involves progressive decline in cognitive functions such as declarative memory or selective attention. Functional magnetic resonance imaging (fMRI) has been used to study the neural correlates of these altered cognitive processes [2]. The majority of these studies focused on AD-induced changes of regional brain responses to cognitive tasks or stimuli. For example, patients with AD activate less in the hippocampus during declarative memory tasks, or they have consistently increased activations in the medial parietal cortex during attention demanding tasks [3-6]. However, the brain is also active in the absence of explicit input and output [7, 8]; furthermore, this so-called resting-state activity is evidently relevant for task-related activity, perception, and behavior [9-12]. Bearing in mind this background, recent fMRI-based findings of AD-associated changes in resting-state activity are of special interest for the study of neural correlates of cognitive symptoms in AD [13-16].

To better understand the motivation for exploring resting-state or spontaneous brain activity, it is useful to have a look at both brain energy metabolism and the relationship between resting-state activity and task states. First, in the resting-state the brain consumes about 20% of the total energy use of the body; about 80% of this brain energy is devoted to synaptic signaling at rest. Compared with at-rest metabolism

task-related increases of brain energy consumption are small (< 5%) [17, 18]. From this cost-based analysis of the brain's functional activity it seems reasonable to conclude that spontaneous brain activity and its changes in AD play a prominent role in the brain's overall function and dysfunction, respectively. Second, several findings point to the relevance of regional spontaneous activity for stimulus-related event performance. For instance, Fox and colleagues demonstrated for the somatomotor system that during right index finger tapping the spontaneous activity in the right motor cortex accounts for the trial-to-trial variability of both the fMRI signal responses in the left motor cortex and the button press forces [10, 11]. Other studies have produced similar results for pain perception or attentional lapses in cognitive tasks [9, 12]. Translated into the context of brain diseases, the influence of spontaneous brain activity on behavior indicates that changed spontaneous brain activity might be relevant for clinical symptoms [19].

Spontaneous brain activity is organized by synchronized oscillations at different temporal and spatial scales [7]. Temporal correlations between low frequency oscillations of fMRI signals derived from distinct brain areas at rest reflect spatial aspects of this organization. Biswal *et al.* were the first to discover this kind of at-rest functional connectivity for the somatomotor system [20]. So-called resting-state networks (RSNs), which are characterized by spatially consistent, functionally connected fMRI signal oscillations between remote brain areas, have since been reported for many functional systems such as the motor, primary sensory, language, attention, and default networks [17, 21-24]. This organization of RSNs seems to be selectively changed in AD [13, 15]; additionally, at other spatial scales than the inter-

*Address correspondence to this author at the Department of Psychiatry, Klinikum rechts der Isar, Technische Universität München, Ismaninger Strasse 22, 81675 Munich, Germany; Tel: ++49-89 4140 4683; E-mail: c.sorg@lrz.tum.de

regional-scale, AD-induced alterations of synchrony-based cerebral organization are detectable by resting-state fMRI [14, 16]. Based on these findings, resting-state functional connectivity MRI (rs-fcMRI) turns out to be an attractive tool to address questions like how cognitive deficits are related to changed network activity, or why certain brain networks are more vulnerable to AD-related pathology than others [25-29].

In this review we focused on studies exploring the functional connectivity (FC) of spontaneous brain activity (SBA) in AD using rs-fcMRI. As a literature search strategy, we used the topics Alzheimer's disease/mild cognitive impairment in combination with resting state/default mode/deactivation. Additionally, each search was restricted by including the topic functional MRI. The review is introduced with a summary on the neural correlates of spontaneous fMRI signal oscillations in order to allow the reader a critical evaluation of the presented results. We brought together studies that explored AD-induced changes of SBA at *three distinct* spatial scales, starting at the inter-regional level (section 2) with a focus on the default network (DN) and continuing with the large-scale level of functional connectivity (section 3) and a final section (section 4) devoted to the regional level. Due to the relative novelty of the presented approach to AD, we emphasized the description of methods used. This approach structures each section in methods, results, and conclusions.

To foreshadow results, we found that AD-induced changes of functional connectivity at rest are particularly prominent in posterior areas of the DN and the medial temporal lobes, and that these changes were present at all spatial scales of analysis and at very early stages of the disease. In the following - for the sake of simplicity and disregarding subtle differences - we will use the terms 'spontaneous brain activity', 'intrinsic brain activity', and 'resting-state activity' synonymously. Here each term refers to brain activity during task-free or resting states, which are characterized as awake states without experimental manipulation of sensory or motor processing.

SECTION 1: NEURAL CORRELATES OF SPONTANEOUS BOLD FLUCTUATIONS

Most fMRI studies rely on imaging the blood oxygenation level dependent (BOLD) signal [30]. BOLD-fMRI measures hemodynamic changes that are linked to underlying neural activity. In order to use fMRI as a tool to study spontaneous brain activity, it is essential to understand the relationship between spontaneous BOLD fluctuations (SBFs) and spontaneous neuronal activity. In the following we will shortly review some key results that concern neuronal correlates of stimulus-induced BOLD responses. After that we will discuss studies focusing on neuronal correlates of SBFs in more detail.

Neural Correlates of BOLD Responses

The local increase of neuronal activity induces a slightly delayed increase of local cerebral blood flow (peaking ~ 6s after the increase of neuronal activity), which exceeds the increase of oxygen consumption, resulting in reduced deoxygenated hemoglobin levels and increased BOLD signal [31-33]. Simultaneous measurements of single- and multi-

unit activity of a small population of neurons along with local field potentials (LFPs) and BOLD contrasts were made in the visual cortex of anesthetized monkeys [33, 34]. The amplitude of BOLD responses was a linearly increasing, but not time-invariant, function of the single- and multi-unit spike activity, and LFPs. Comparing the predictive values of spike activity and LFPs, LFPs performed slightly better than multi-unit activity. Additionally, in certain circumstances LFPs and spike activity can be dissociated; in these conditions only LFPs predict BOLD responses [34, 35]. Taken together, the LFPs seem to be the key predictor of the BOLD response, indicating that BOLD activity seems to primarily reflect the input and local processes of neuronal information, i.e. synaptic activity, rather than the output signal of projecting neurons, i.e. spike activity.

Neural Correlates of SBFs

Most evidence for the neural nature of SBFs is derived from four sources: spatial comparisons of SBFs with anatomically defined structural networks in nonhuman primates as well as in humans, simultaneous recordings of intra-cortical neuronal activity and BOLD activity, simultaneous EEG-fMRI, and finally lesion studies that will be extensively discussed in the context of AD in later sections. First, in macaque monkeys, Vincent *et al.* detected an oculomotor control-related RSN, which is a potential homologue to a human RSN and which largely coincides with anatomical connectivity patterns labeled by retrograde tracer injections [36]. Second, in humans, substantial correspondence between the structural and functional connectivity of the DN was measured by DTI and rs-fcMRI [37]. Third, Shmuel and Leopold revealed correlations between SBFs and underlying local neuronal activity in the visual cortex of anesthetized monkeys using simultaneous intra-cortical neurophysiological recordings and fMRI [38]. With a time lag of about 6s, SBFs were locally related to neuronal spiking rates and to relative power changes in the multi-unit activity band and most prominently in the LFP gamma-band (see Fig. (1)). Furthermore, the study demonstrated that SBFs of remote areas of both visual cortical hemispheres were correlated to a single recording site of neuronal activity in V1. Both results together strongly support the neural origin of regionally and inter-regionally synchronized SBFs. Fourth, a few studies using simultaneous EEG-fMRI explicitly assessed SBFs. SBFs are synchronized across remote brain areas, comprising above-mentioned RSNs. When the subject has her eyes closed, posterior EEG power in the alpha-band is inversely related to SBFs in the occipital, superior temporal, cingulate, and inferior frontal cortex [39-41]. Mantini *et al.* found characteristic and replicable EEG-band signatures for distinct RSNs [42].

Summary 1

Taken together, SBFs seem to reflect both structural and dynamic aspects of neuronal activity (for more detailed discussion see [17]). Whether additional plastic aspects of neuronal activity are represented in SBFs is presently not well understood [43, 44].

In the following we will discuss AD induced changes of synchronized SBFs at distinct spatial levels. We start with the inter-regional level.

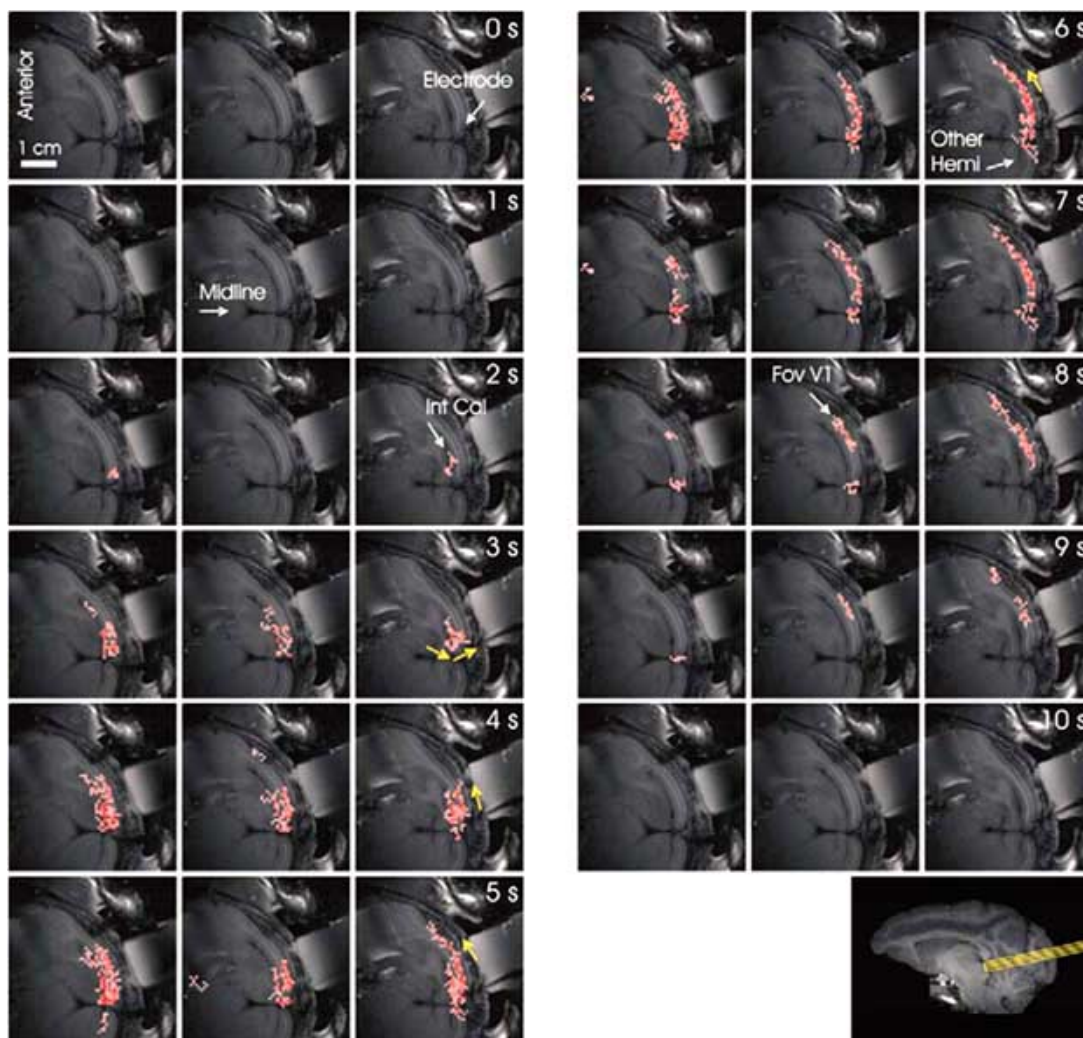


Fig. (1). Spatio-temporal evolution of the correlation between fluctuations in BOLD and neuronal activity. Each row represents 3 axial T1 images of the right occipital cortex of a monkey; the exact location of images is shown in the picture right below; in each image right above the holder of the electrode is depicted. The figure presents the correlation between the slow relative fluctuations in power averaged over frequencies of the neuronal signal recorded at the tip of the electrode (white arrow) and the fluctuations in BOLD measured voxel-by-voxel. The labels “0 s”, “1 s”, . . . “10 s” mark the lag between BOLD and neurophysiological signals used for the computation of the corresponding correlation images. Pink colored voxels showed statistically significant positive correlation between the neurophysiological and BOLD signals for the corresponding time-lag. The further white arrows point to the midline, the internal calcarine sulcus (“Int Cal”), to the hemisphere contra-lateral to the electrode (“Other Hemi”) and to the central visual field representation in V1 (“Fov V1”). The yellow arrows point to the direction of propagation of the correlation along the gray matter. Adapted with permission from data published in Shmuel A. and Leopold D. [38].

SECTION 2: AD-INDUCED CHANGES OF THE INTER-REGIONAL SYNCHRONY OF SPONTANEOUS BRAIN ACTIVITY

Methods for the Detection of Inter-Regionally Synchronized Spontaneous BOLD Fluctuations

Resting state conditions such as visual fixation on a cross-hair or keeping the eyes closed without falling asleep are appropriate conditions to examine SBFs with fMRI. After data acquisition, data sets are cleaned of non-neuronal noise, and subsequently analyzed for spatial patterns of inter-regionally synchronized SBFs. Non-neuronal noise comprises scanner-induced noise and physiological noise such as respiratory or cardiac activity induced BOLD fluctuations [23, 45]. Several methods effectively account for non-

neuronal noise reduction: For example, band pass filtering is used to remove scanner drift related signals; physiological parameters like respiratory activity can be monitored during BOLD data acquisition with subsequent removal of these parameters by linear regression [45]; in the BOLD data analysis itself non-neuronal noise isolation can be performed by regressing out signals common to all voxels (global signal) or from non-neuronal noise-sensitive regions like white matter or ventricles [46-48]. Using independent component analysis (ICA, for more detail see below) it is possible to separate noise-related from neuronal activity-related processes [15, 23].

For the detection of spatial patterns of inter-regionally synchronized SBFs region-of-interest (ROI) based correla-

tion approaches are the most frequently used techniques [20, 17]. Essentially, the averaged time-course of the BOLD signal of an a priori defined seed region is extracted and then correlated with the signal time-courses of all other brain voxels (see Fig. (2)). Significantly correlated voxels generate a map of regions, which are synchronized in their spontaneous BOLD activity with respect to the selected ROI. Advantages of this approach are its sensitivity and its ease of interpretation. However the analysis is restricted to seed regions with strong a priori criteria and any participation of the seed region in distinct networks is hard to detect from the averaged BOLD time-course. Accounting for these limitations, graph-theoretic methods and ICA have additionally been used [21, 49, 50]. Graph-theoretic methods, which are based on the pair wise signal time-course correlations of many a priori selected ROIs, will be presented in detail in section 3. ICA, the second most popular technique for analyzing resting state fMRI data, enables the separation of the data set into independent components by using algorithms like the INFOMAX algorithm [50-52]. Resulting components are independent in a statistical sense, or in other words statistical independence is the criterion for the component separation. Each component comprises a spatial map and an according component-related time-course (see Fig. 3 for several spatial maps, time courses are not depicted). In a subsequent step information about the cortical localization of the spatial maps and their temporal profile is used to sort components into presumably neuro-anatomical systems and noise related processes. In the following we have restricted our review to rs-fcMRI studies using ROI-based correlation methods or ICA for the detection of RSNs in AD. For the sake of clarity we start with ROI-based studies.

ROI-Based Correlation Analyses of SBFs in AD Set the Stage: Focus on the Default Network

The medial temporal lobes (MTL), including the hippocampus (HC), were the first regions to be used for ROI-based functional connectivity analyses of the resting-state in AD [53, 54]. This set of regions is already affected in early stages of the disease [1]. Deposition of neurofibrillary tangles, increasing atrophy, and reduced activity during declarative memory tasks have been consistently reported for areas of the MTL [2, 55, 56]. Regarding at-rest functional connectivity of the MTL in healthy controls, Kahn and colleagues found that the anterior HC and the entorhinal cortex are functionally connected with the lateral temporal cortex extending to the temporal pole, whereas the posterior HC and parahippocampal cortex are mainly linked to the medial prefrontal cortex (mPFC), the posterior cingulate, retrosplenial, and lateral parietal cortex (PCC, RSC, LPC) [57]. PCC, mPFC, and LPC together constitute the core regions of the so-called default network (DN), which is severely affected by AD (discussed in detail below) [58].

Liang Wang *et al.* were the first who explicitly compared the hippocampal FC-patterns at rest between patients with mild AD (n=13) and age-matched healthy controls [54]. Seed regions were the left and right HC – no distinction between anterior and posterior parts of the HC was made. The authors found prominently reduced FC of the right HC to all key regions of the DN as well as to small lateral temporal areas. Interestingly, the left HC showed increased FC to the right lateral PFC, possibly representing compensatory mechanisms. In a similar study of Allen *et al.*, assessing 8 patients with mild to moderate AD, patients presented a more disseminated pattern of reduced HC-related FC, includ-

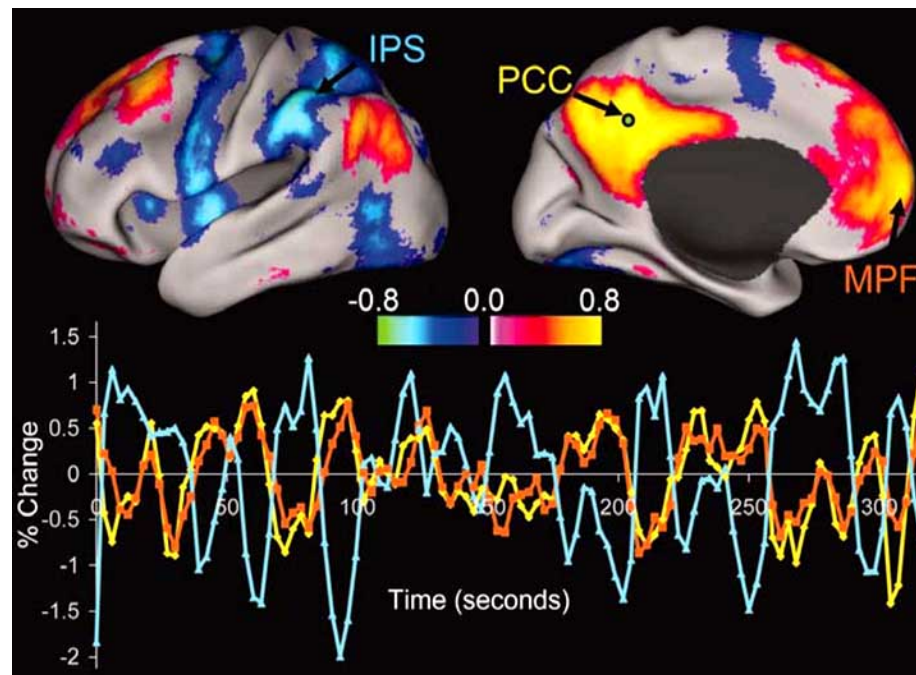


Fig. (2). Correlations between a seed region in the PCC and all other voxels in the brain for a single subject at rest. The spatial pattern of correlation coefficients shows both correlations (positive values) and anti-correlations (negative values), thresholded at $R = 0.3$. The time course for a single run is shown for the seed region (PCC, yellow), a region positively correlated with this seed region in the medial prefrontal cortex (MPF, orange), and a region negatively correlated with the seed region in the inferior parietal sulcus (IPS, blue). Adapted with permission from data published in Fox *et al.* [46].

ing distributed neocortical and cerebellar areas with completely diminished connectivity to prefrontal sites [53]. Explanations of the partly inconsistent results of both studies are related to differences in the disease severity of assessed patients, in the statistical power of both analyses (different group sizes), and in the methods of ROI definition.

In a further ROI-based study Kun Wang and colleagues divided the brain into 116 ROIs and investigated AD-induced changes of each pair wise ROI-ROI-correlation in healthy elderly (n=17) and patients with mild AD (n=17) [59]. Without correcting for the rather large number of comparisons the authors found for the AD group indications for reduced long-range connectivity between areas of the prefrontal and parietal cortex as well as increased short-range FC between areas within the frontal, parietal, and occipital lobes. When constraining the analysis to the FC-pattern of the PCC as a key region of the DN, positive correlations with areas within the DN and negative correlations with areas, which are routinely recruited during a wide range of attention demanding tasks, were significantly reduced in the AD group.

Two important points can be derived from these studies: first, in AD the functional connectivity of the DN at rest seems to be reduced in three ways: within the DN in relation to the PCC, in its relation to the MTLs, and in its interplay with attention-relevant areas of the frontoparietal cortex. Second, the large-scale organization of synchronized SBFs seems to be changed in AD, even if other methods than pure ROI-based correlation techniques are needed to map these changes (see section 3).

Due to its prominent relevance in AD, we insert a short description of the DN in the next paragraph.

Parenthesis: The Default Network and Negatively Correlated Functional Networks

First evidence for the existence of the DN as an anatomically defined brain system comes from the observation of spatially consistent patterns of deactivation in the PCC, LPC, and mPFC (for an excellent review, see [60]). Deactivation in the context of neuroimaging refers to the reduced activity of an area during task-related events/states compared to control or rest states. Areas of the DN consistently deactivate across a wide range of attention demanding tasks, independent of the exact task design and of the used imaging method, e.g. PET, blocked- or event-related fMRI [58, 60]. The DN also constitutes itself as a RSN of synchronized SBFs [61] (see Fig. 2). Furthermore, SBFs of the DN are anti-correlated to the SBFs of a widely distributed set of regions commonly activated in attention related tasks. This last fact indicates an intrinsic organization of the brain into anti-correlated functional networks, which seems to be changed in AD (regarding AD see the results of Kun Wang *et al.*; yet, see below for an ongoing discussion about the reliability of anti-correlated networks) [15, 46, 47]. During tasks of varying attentional load the degree of stimulus-independent thoughts is correlated with the degree of activity in the DN [62, 63]. Finally, regions of the DN themselves are engaged in functions like remembering episodic events, planning future events, imagining spatial relations, and understanding the mental states of others – in short, navigating in time, space and social affairs for distinct purposes [60, 64].

Several hypotheses have so far been formulated to integrate these distinct findings, yet differing in their account for distinguishing task- and non-task/rest states. Task states are characterized by focused attention and task-related mental content, non-task states by environment-related attention and wandering mental content. One class of approaches explaining the function of the DN emphasizes attentional changes: they relate DN activity to low-level attention that scans the environment for potential dangers [65]. Another class of hypotheses emphasizes the changes of mental content in task- and non-task states: e.g. Buckner and colleagues suggest that the DN is routinely engaged in the constructive imagination of events, based on past experiences and adaptive for future navigating in events and social interactions; this approach explicitly accounts for the intimate relation of the episodic memory related MTL system to the DN, a relation that is prominently changed in AD (see above and below [54, 66, 67]).

Above we mentioned the observation that spontaneous BOLD fluctuations within the DN seem to be negatively correlated with fluctuations of a widely distributed assembly of regions usually involved in attention-demanding tasks [15, 44, 46, 47, 68]. There is an ongoing discussion whether this finding is real or an artifact of image preprocessing methodology [69-71]. Global BOLD signal fluctuations, which are common to all voxels of the brain, have to be removed by preprocessing to detect negatively correlated BOLD signals at rest. Global fluctuations are suggested to represent noise signals like movement, respiration, cardiac pulsation or global arousal. Murphy *et al.* demonstrated in simulated and real rs-fMRI data sets that global signal procedures could produce artificially negative correlated networks [71]. However, Fox and colleagues used simulated rs-fMRI data to adapt their previous account on global signal regression [46, 69]; they used the adjusted procedure to reanalyze human data of their previous study and found that previously observed negatively correlated brain networks were consistent with a true physiological negative correlation as opposed to an artifact of global regression. Furthermore, we consistently found negative correlations between the DN and the attention-related network using model-free ICA of rs-fMRI data, which were not regressed for global signal [15]. Future studies are necessary to better evaluate the effects of global signal regression. Stated carefully, global signal regression is a useful tool for preprocessing rs-fMRI data with the disadvantage of generating interpretation problems for negatively correlated signals; anticorrelated functional networks seem more likely to reflect real physiological relations than methodology-derived artifacts.

In the following these facts about the DN constitute the background for interpreting AD-induced changes of the DN.

AD-Induced Changes of the Default Network in the Context of Resting-State Activity: Deactivation Deficits and Reduced Intrinsic Functional Connectivity

Deactivation processes of the DN are, by definition, indirect measurements of the baseline/resting state activity of the DN. Several findings report on changed DN deactivation in

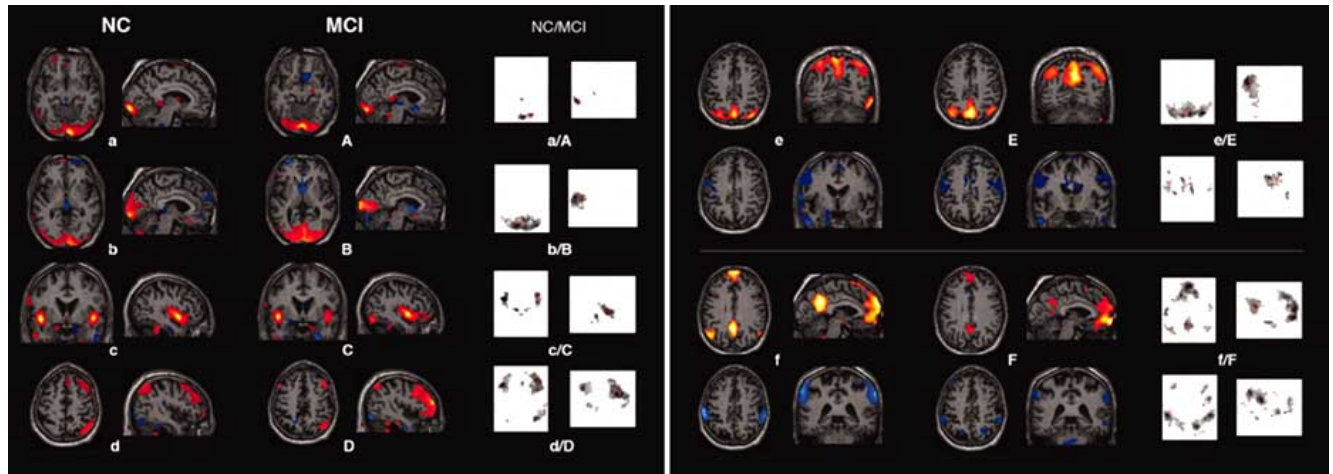


Fig. (3). Group-level RSNs of normal controls (a-f) and patients with amnesic MCI (A-F). Each group IC image contains a pair of spatial IC-patterns, representing voxels that are correlated (red) or anti-correlated (blue) to the component's time-course (not shown). For IC images a/A to d/D each pair of IC-patterns is shown within one brain image; for IC images e/E and f/F each upper row represents the correlated IC-pattern, each lower row the anti-correlated one. IC patterns are superimposed on a single subject high resolution T1 image. The black to yellow/light blue colour scale represents z-values, ranging from 1.8 to 8.0. Glass brain projections illustrate results of one-sample t-tests on the individual back-reconstructed subject IC-patterns across both groups ($p < 0.05$, FDR corr.). For ICs a/A to d/D one-sample t-test on the anti-correlated individual subject IC-patterns provided no significant results. In axial view the right hemisphere is displayed on the right. NC, normal controls. Adapted from data published in Sorg *et al.* [15].

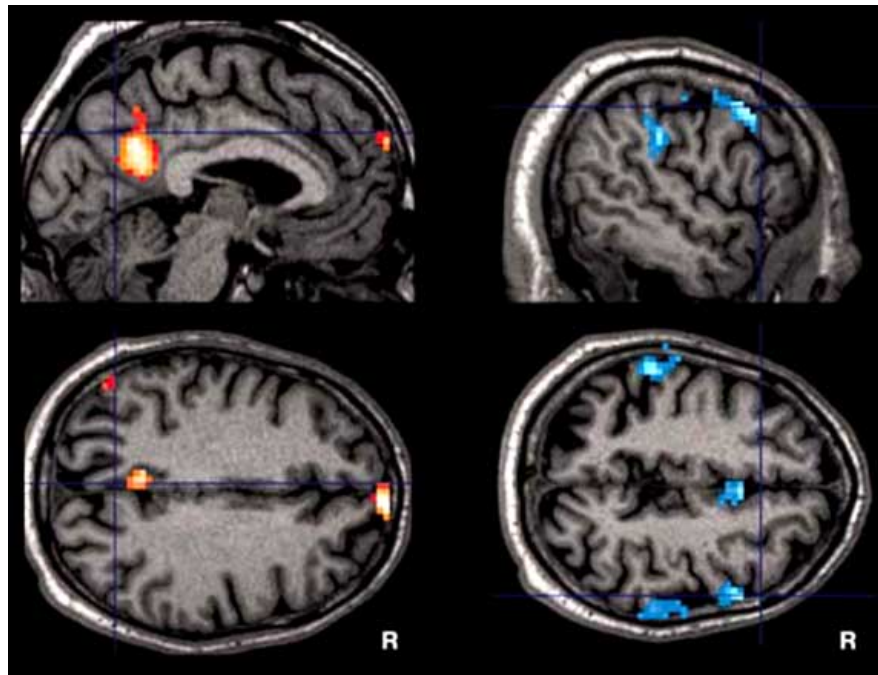


Fig. (4). Contrasts of RSNs between normal controls and patients with amnesic MCI. Left maps correspond to the DN of upper Fig. (3) f/F and right maps to the executive attention networks of lower Fig. (3) f/F. Colour maps represent significant ($p < 0.05$ FDR corr.) voxels of higher component related activity in controls compared to patients. Corresponding t-values are colour-coded with black to yellow (from 0 to 5.0) or to light blue (from 0 to 6.2), respectively. Maps are superimposed on a single subject high resolution T1 image. The patient group did not show any significant higher activation for DN or the executive attention network, respectively. For all remaining RSNs of Fig. (3) two-sample t-tests did not reveal any significant difference between the two groups. R, right hemisphere. Adapted from data published in Sorg *et al.* [15].

AD. During alternating blocks of a semantic classification task and rest, Lustig and colleagues found a reduced magnitude of deactivation in the PCC of AD-patients compared to healthy elderly in fMRI data [5]. Furthermore, the temporal

profile of the response in the PCC to a task quickly reversed its sign in young controls, whereas in AD activation was maintained throughout the task blocks. Rombouts and colleagues demonstrated a similar result for patients with mild

cognitive impairment (MCI) during an encoding and spatial working memory task [6]. The main differences between healthy elderly and patients occurred in the early phase of deactivation in the mPFC and posteromedial cortex (PCC and retrosplenial cortex), reflecting a reduced reactivity and adaptation of the DN. Across the spectrum from healthy elderly over MCI to mild AD the degree of deactivation in the PCC during encoding was correlated with memory performance within and outside the scanner [72]. Furthermore, for patients with MCI, PCC deactivation during encoding predicts the risk of cognitive decline, especially the conversion to dementia [73]. Taken together, areas of the DN deactivate less in magnitude and responsiveness along progressive AD, the degree of deactivation deficits is task- and AD-severity-dependent, and frontal and parietal areas behave distinctively with stronger AD-related changes in the PCC.

Focusing on the intrinsic functional connectivity of areas that usually deactivate during attention-demanding tasks, Greicius and colleagues found synchronized SBFs between the mPFC and the PCC during rest and a low-level sensory task. This study was the first demonstrating that the DN might be a RSN [61]. In a second study, in order to evaluate the whole set of co-activating regions in the DN and their changes in AD, the authors used ICA to examine SBFs in areas of the DN in healthy elderly and in patients with mild AD [13]. Reduced co-activation in the DN was found in the AD group for the PCC, LPC, mPFC, and the HC; the HC was integrated in the DN across both groups, reflecting its intimate relation to the DN. Furthermore, a goodness-of-fit analysis of individual DN patterns suggested that DN activity at rest might be a potential biomarker for incipient AD. This study was the first that found evidence for the notion that rs-fcMRI might serve as a functional bio-imaging marker that distinguishes healthy controls from patients.

AD-Induced Changes in the Plurality of RSNs

The results of the second study by Greicius and colleagues inspired some further questions: are even more RSNs altered in AD than the DN? Do changes already occur in patients with MCI? How do potential FC changes relate to atrophy? And lastly, do integrated imaging scores, which rely both on functional and structural changes of RSNs, better distinguish controls from patients than isolated scores? To address these questions, we examined 24 patients with MCI and 16 healthy controls with structural and functional MRI at rest [15]. ICA of the fMRI data revealed decreased FC only for selected areas of the DN and the executive attention network in the patient group while the remaining RSNs were unaffected (Figs. (3) and (4)). Both networks were anti-correlated in their activity across time. Voxel-based morphometry identified atrophy in both MTLs of the patients. Areas of reduced co-activation did not overlap with areas of reduced grey matter. Using an additional ROI-based correlation approach, the functional connectivity between both HCs in the MTLs and the posterior cingulate of the DN was present in healthy controls but absent in patients. Furthermore, when accounting for both structural and functional information (HC volume, ROI-based FC between HC and PCC), patients could be better distinguished from controls than when including only one type of information. This result

supports the idea of integrated bio-imaging markers in prodromal AD (Fig. (5)).

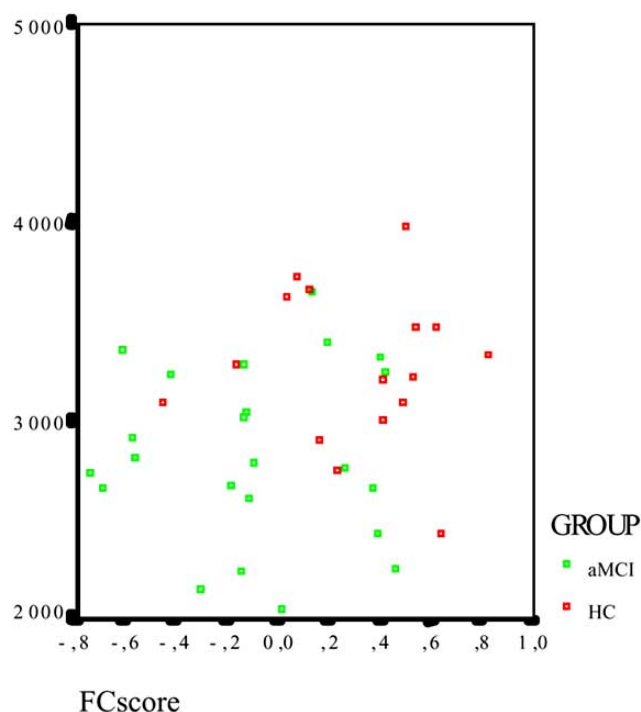


Fig. (5). Shows the relation between a structural *VBM score* and a functional *FC score* with an additional classifier. The *VBM* approach allows us to calculate the hippocampal volume in each individual. The anatomical data set consists of two scalar values for each individual representing the volume in [ml] of the left and the right hippocampus. The mean value of this score is titled *VBM score*. The *FC score*, represents the correlation coefficient [z-score] between the signal time-courses of the hippocampus with the PCC. The blue classifier indicates that the scores taken together allow for a better discrimination of the group of patients than does a singular score. HC, healthy control, aMCI, amnesic mild cognitive impairment.

SUMMARY 2

First, following an approach to AD which focuses on the functional connectivity of spontaneous brain activity at the inter-regional level, most AD-induced changes were found in the posterior DN: decreased FC within the DN [13, 15, 59], in relation to the MTLs [13, 15, 53, 54], and in relation to a widely distributed set of regions usually recruited in attention-related tasks [15, 59]. Furthermore, the deactivation dynamic of the posterior DN seems to be impaired, enabling predictions for the further disease process [5, 6, 72, 73]. At last, these findings are not restricted to patients with AD – patients with MCI are also affected.

Second, the results of Kun Wang *et al.* and Sorg *et al.* suggest that AD-related changes of FC might affect multiple cortical systems [15, 59]. Whether AD influences more global features of cortical network organization is the guiding question of the next section.

SECTION 3: AD-INDUCED CHANGES OF THE LARGE-SCALE ORGANIZATION OF SYNCHRONIZED SPONTANEOUS BRAIN ACTIVITY

Small Worlds and Graph Theoretical Methods

The fundamental idea of a small world organization for a given structure can be easily illustrated by the organization of social networks. Our close friends and relatives compose a cluster of social contacts; two of my friends are often also friends of each other. However, when traveling to a distant city we sometimes make the experience that some of the new people we meet are socially connected with someone we already knew (friends of friends). The number of social relationships between any two people can be very small in comparison with the size of the population [74]. Watts and Strogatz were the first who formalized these familiar concepts in graph theoretical terms, enabling applications of quantitative complex network analysis that have been extended to systemic neuroscience [75]. Formalized as a graph, members of a social network are represented by the graph's nodes, while the connections between them (i.e., friendships) are represented by edges connecting the nodes. The small world concept describes a type of graph in which nodes are separable into clusters (with lots of connections among the members of the clusters), which are linked to other clusters via a small number of connections. There are several obvious reasons why the brain might be organized as a small world network: First, the brain, as a complex network which is hierarchically organized on multiple temporal and spatial scales, supports both segregated and distributed processing; small world topologies realize both local clustering, corresponding to regional segregation, and short path length between any two nodes across the network, which is compatible with distributed integrated processing [74]. Second, brains evolved to maximize functional efficiency and to minimize connectivity costs; small world topologies enable both high local and global efficiency in distributed parallel processing and sparse connectivity between nodes, i.e. low wiring costs [76].

In large-scale cortical networks nodes typically represent distinct cortical regions and edges represent inter-regional pathways. Inter-regional pathways refer to parameters characterizing structural or functional connectivity, e.g. the size of white matter tracts connecting the regions or the correlation coefficient between their signal time courses, respectively. A symmetric correlation matrix is often used to create a graph representing connection strengths across the entire cortex (see Fig. (6)). To characterize a given node i in a network, one might measure its *degree* k_i (the number of nodes to which it is directly linked), the *path length* L_{ij} to another node j (the number of edges in the shortest path between those two nodes), and its *clustering coefficient* C_i (the proportion of neighbor-pairs that are directly linked to one another, forming a triangle; think of two of your friends, who are also friends of each other). Based on these individual node measures, one can then define properties of the entire network structure (i.e. the entire cerebral cortex) and classify networks based on their overall properties. The degree distribution of a graph is its probability distribution of k . For example, a random graph has an exponential degree distribution: $P(k) = \exp(-ak)$. To study the properties of a given network, the *minimum path length* L and *clustering coefficient* C of the whole network are calculated by averaging over all L_{ij} and C_i ; L and C are subsequently compared with according L_{rand} and C_{rand} of a *random network* that has the same degree distribution, number of nodes, and edges as the network of interest. For *small world networks*, which show a balance between high average clustering and relatively short distances between nodes, the ratio $\lambda = L/L_{\text{rand}}$ is expected to be ~ 1 , while the ratio $\gamma = C/C_{\text{rand}}$ should be greater than 1.

cient C of the whole network are calculated by averaging over all L_{ij} and C_i ; L and C are subsequently compared with according L_{rand} and C_{rand} of a *random network* that has the same degree distribution, number of nodes, and edges as the network of interest. For *small world networks*, which show a balance between high average clustering and relatively short distances between nodes, the ratio $\lambda = L/L_{\text{rand}}$ is expected to be ~ 1 , while the ratio $\gamma = C/C_{\text{rand}}$ should be greater than 1.

The Large-Scale Organization of Synchronized SBFs is Characterized by Small World Properties

Achard, Bullmore, and colleagues were the first that demonstrated the small world organization of SBFs in humans [49]. Rs-fcMRI data of healthy controls were separated into 90 cortical and subcortical regions. For each region and each subject the regionally averaged signal time courses were calculated and wavelet transformed. Wavelet transformation results in a time-scale decomposition of the averaged signal that partitions the total signal energy over a set of little waves, each of which is uniquely scaled in frequency and located in time [77, 78]. Six frequency scales totally ranging from 0.007Hz to 0.45Hz were defined and for each scale and for each regional pair the inter-regional correlations between wavelet coefficients were calculated. This procedure results in a set of six (90 x 90) inter-regional wavelet correlation matrices for each subject, which were averaged over subjects at each scale to produce six group mean wavelet correlation matrices (Fig. (6)). To create graphs/networks from each correlation matrix, each correlation r was tested for $r > R$ with subsequent correction for multiple comparisons. The value R , which works as the threshold for a given wavelet correlation matrix, was selected as maximum value R , for which small world properties are estimable, as defined by the theory of complex network analysis [75]. Small world topology with sparse connections was found for the low-frequency interval 0.03-0.06Hz with a global mean path length of 2.49, which is equivalent to a comparable random network, and with a local clustering coefficient of 0.53, which is two times greater than in the according random network. Similar parameters were found for anatomical connections in the macaque cortex [79]. Regions with a high degree of significant connections mainly consisted of recently evolved regions of the heteromodal association cortex, with long-distance connections to other regions. Regions of the unimodal association and primary cortices were more cliquishly connected. Paralimbic and limbic regions were less intensively connected than hubs of the association cortex. In conclusion, SBFs hold a small world organization that probably reflects underlying anatomical architecture [37]. The question arises whether AD changes this basic organization of synchronized SBFs.

AD Changes the Small World Organization of the Brain

Supekar, Greicius, and colleagues answered this question by following the approach of Achard *et al.* [16]. They examined 21 patients with AD and 18 healthy controls by rs-fcMRI. After whole brain separation into 90 regions, wavelet transformation, and calculation of the (90 x 90)-correlation matrix, a small world structure was found for both groups of healthy controls and patients with AD, most prominently in the frequency interval 0.01-0.05Hz. For this frequency range

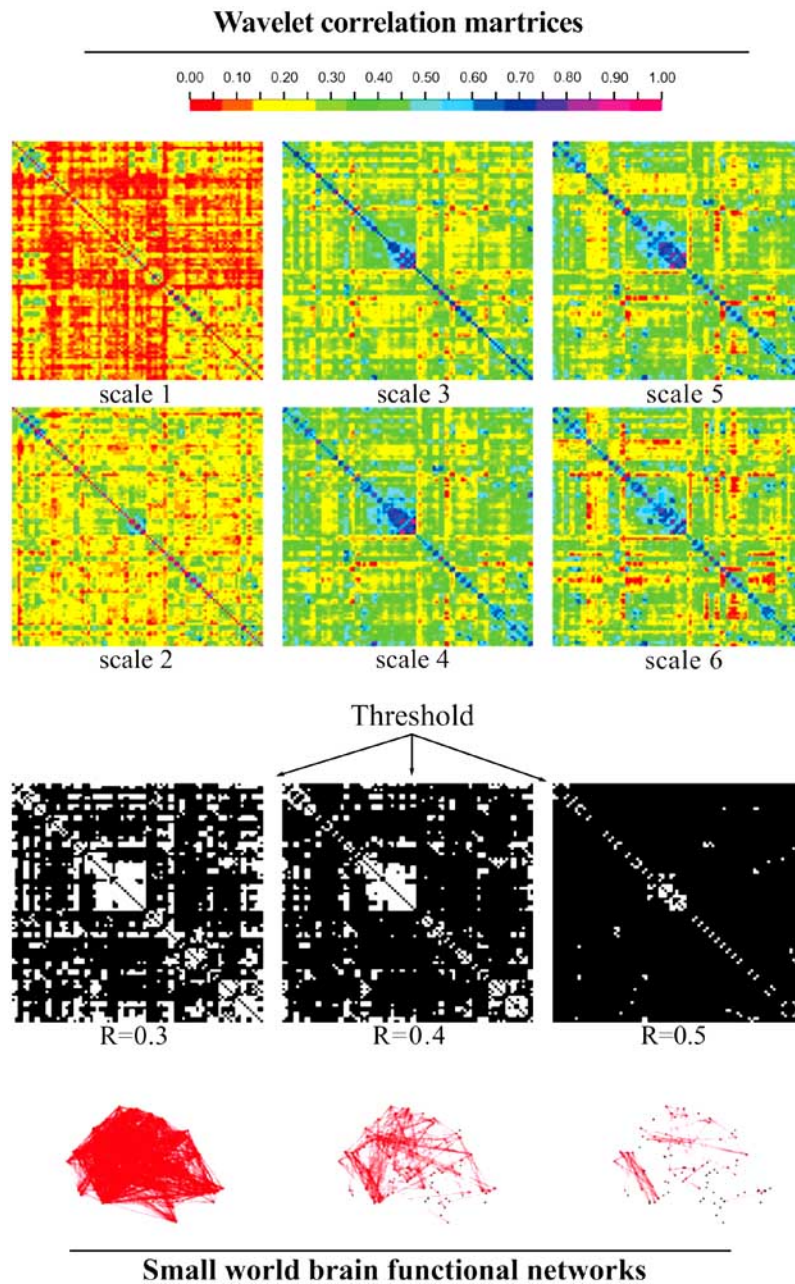


Fig. (6). Schematic of wavelet correlation analysis, thresholding, and functional network visualization. *Top:* fMRI time series recorded from each of 90 regions in each subject are decomposed using the wavelet transformation, and the inter-regional correlation is estimated at each frequency scale for each pair of regions in each subject; individual wavelet correlation matrices are then averaged over subjects at each scale to produce a set of six group mean wavelet correlation matrices. *Middle:* The wavelet correlation matrices are thresholded to generate binary matrices, each element of which is either black (if there is no significant connection between regions) or white (if there is). The stringency of the probabilistic thresholding operation is determined by the value of the correlation threshold R , as illustrated by applying three different thresholds ($R = 0.3, 0.4, 0.5$) to the scale 4 wavelet correlation matrix. *Bottom:* Thresholded matrices are visualized in anatomical space by locating each region according to its y and z centroid coordinates in Talairach space and drawing an edge between regions that are significantly connected. Adapted with permission from data published in Achard *et al.* [49].

group comparisons of small world metrics revealed that the local clustering coefficient was significantly reduced in the patient group, indicating disrupted local connectivity in AD. Both hippocampi demonstrated especially reduced clustering in the AD group. The characteristic path length was not significantly different across groups. Furthermore, the clustering coefficient distinguished AD patients from the controls

with high sensitivity (72%) and specificity (78%), suggesting that these network measures may be useful as an imaging-based biomarker to distinguish AD from healthy aging.

Similar results of changed small world topology in AD have been reported by He and colleagues and Stam and colleagues using structural MRI and EEG, respectively [80, 81]. He and colleagues employed a new morphometric technique

to infer anatomical connectivity: correlation patterns in cortical thickness. The assumption underlying this technique is that two cortical areas are likely to be anatomically connected if, after controlling for other factors, their thickness co-varies across subjects. If thickness correlations are produced by shared trophic influences or are due to activity-dependent plasticity, then the inference from thickness correlations to anatomical connectivity is probably well-founded. The authors first calculated cortical thickness correlation matrices for the two groups of 92 patients with AD and 97 healthy elderly. AD patients showed decreased cortical thickness correlations between bilateral parietal regions and increased thickness correlations in several selective regions involving the lateral temporal and parietal cortex as well as the cingulate and medial frontal cortex. Most interestingly here, AD patients showed further abnormal small-world architecture in the structural cortical network with increased local clustering and path length, suggesting a less optimal topological organization in AD. Stam and colleagues used resting-state EEG to study small world properties in healthy controls and patients with AD [81]. Applying analysis methods very similar to those used by Achard and colleagues, they found increased path length and unchanged local clustering in the β -band of AD patients.

SUMMARY 3

AD significantly changes the large-scale organization of SBA; regarding SBFs, beside globally decreased local clustering, both hippocampi demonstrate particularly reduced local cliquish organization. However, the results of studies concerning distinct aspects of brain organization using different methods – rs-fMRI, structural MRI, EEG - do not correspond very well to one another. Partly, these differences might be explained by methodological reasons, e.g. volume conduction in scalp EEG data, which reduces the sensitivity to detect differences in short-range connectivity while enhancing the relative sensitivity to detect differences in long-range connectivity. Results may also differ across methods because different methods assess the organization of distinct processes. For instance, structural MRI maps long-term plasticity, while fMRI maps short-term BOLD activity. Future studies should combine connectivity estimates gathered from distinct, simultaneously used techniques, e.g. thickness correlations, DTI tractography or functional measures, in search of convergent results [82].

After focusing on AD-induced changes of the large-scale organization of synchronized SBFs, we next concentrate on changes of the regional synchrony of SBFs.

SECTION 4: AD-INDUCED CHANGES OF THE REGIONAL SYNCHRONY OF SPONTANEOUS BRAIN ACTIVITY

Methods for Detecting Intra-Regional Integration of Brain Activity

The underlying idea of the concept of cerebral local or (intra)-regional integration is very simple: local brain activity is intensively integrated due to the prominence of local structural connectivity [83, 84]. Locally integrated activity covers both functionally connected and functionally homogeneous activity within a region. This proposal has been recently ex-

plored by Zang *et al.*, who used multiple-time-series measurements of nearby voxels to map local integration, and by Kriegeskorte *et al.*, who showed that improved functional activation maps could be obtained using an information-based approach incorporating the local functional homogeneity instead of spatial smoothing [84, 85]. To characterize rs-fMRI data by regionally synchronized SBFs, at least two distinct approaches can be distinguished. First, some approaches characterize the regional FC of SBFs using Pearson's correlation coefficient (in analogy to ROI-based inter-regional FC). Li and colleagues calculated the mean of voxel-pair cross-correlations to evaluate the regional functional connectivity of the HC [14]. In a follow-up study they extended this approach by examining the mean of phase shifts between voxel time series of a selected ROI (PSI, phase shift index). In contrast to cross-correlation means, phase shifts have the advantage of being independent of the signal-to-noise ratio [86]. Desphande *et al.* generalized the approach of Li and colleagues: they used the integration of the whole spatial correlation function for each voxel instead of the mean of VOI-correlations for a limited number of voxels [83]. The second kind of approach characterizes the local cerebral homogeneity of brain voxels using Kendall's concordance coefficient; Kendall's coefficient of concordance represents a rank correlation measurement, which maps the similarity between data arrays. Zhang *et al.* used this approach to evaluate for each voxel of the brain the mean similarity between the time series of the voxel of interest (VOI) and each time series of limited neighborhood voxels [85].

AD Changes the Regional Coherence of SBA Mainly in Areas of the Posterior DN and the Hippocampus

Using rs-fcMRI, Li *et al.* determined the cross-correlation index (COSLOF) for both hippocampi in 9 healthy controls, 5 patients with MCI and 10 patients with mild AD. Loss of COSLOF, reflecting reduced hippocampal functional synchrony, increased significantly in MCI and mild AD (controls < MCI < AD) [14]. Furthermore, an exponential curve fits the relationship between the COSLOF index and the Mini-Mental Status Examination score (MMSE), indicating a rapid decrease in cognitive capacity once a lower threshold of the COSLOF is passed. In a follow-up study assessing 13 controls, 8 patients with MCI, and 14 patients with mild AD, the phase shift index (PSI) of synchronized hippocampal SBFs was demonstrated to be significantly increased in AD and MCI compared to controls (AD > MCI > controls). Additionally, the authors found that the PSI had a higher group-discriminative power than COSLOF [86]. These results indicate that, the larger the PSI, the less synchronized the SBFs in the hippocampi of patients with AD.

He *et al.* studied the regional homogeneity index ReHo across the whole brain in 14 healthy elderly and 14 patients with AD [87]. Reduced ReHo was found in the posteromedial DN in AD, which remains significant also when controlling for atrophy but with a decrease in statistical power. The loss of statistical power indicates that volume effects are partly reflected in the ReHo index. Furthermore, the PCC-ReHo decrease was correlated with decreases on the MMSE, and increased ReHo was found in bilateral retrosplenial cor-

tex, left fusiform gyrus and right lingual gyrus, which is possibly related to compensatory recruitment. In a further study of Bai *et al.*, using the same methodology as He *et al.* in 20 patients with MCI and 20 controls, the posteromedial DN was again significantly reduced in its ReHo, even after controlling for atrophy. Increased ReHo was found in the right inferior parietal and right fusiform cortex [88].

SUMMARY 4

Two distinct types of measurements have been defined to characterize regional integration processes by rs-fMRI. Decreased intra-regional synchrony of SBFs was found in the hippocampi of patients with AD and MCI. Decreased regional homogeneity of SBFs was found in the medial parietal DN of patients with AD and MCI.

CONCLUSIONS

Approaching AD with rs-fcMRI to explore changed synchrony of spontaneous brain activity leads us to four conclusions. First, focusing on the regional aspect, mainly areas of the posterior default network and the medial temporal lobes are affected. Second, within these areas the neuronal communication between distinct brain areas is at least impaired at three levels of organization: the regional, inter-regional, and large scale. Third, most of these changes are already found in patients with mild cognitive impairment. Fourth, rs-fcMRI has the potential to define functional bio-imaging markers to distinguish healthy aging and early AD.

For future research these conclusions trigger at least three questions. First, how do FC-changes of SBFs of distinct levels relate to each other? For example, the posterior-DN-MTL system is predominantly affected by reduced inter-regional functional connectivity in early AD, but it is unclear how these apparently spatially limited changes relate to changes of large-scale organization and how this relation evolves along the course of AD. Second, can AD be understood as a disorder of the DN-MTL system [25, 29]? Several theories have tried to explain the spatial pattern of neuropathological changes – neurofibrillary tangles and amyloid plaques – across the brain, ranging from models focusing on the region-specific anatomy to hypotheses favoring regional differences in plasticity [89-91]. Due to the large concordance between the spatial distribution of amyloid plaques and the DN, Buckner and colleagues formulated the so-called metabolism hypothesis of AD. The metabolism hypothesis relates the prominent role of amyloid plaques to DN-MTL function in order to explain the origins of AD: the preferential use of the DN and the closely related MTL-system throughout life, i.e. the memory-based imagination in different functions and mainly during rest, “may be conducive to increased accumulation of A β and its pathological sequelae. By this view, memory systems may be preferentially affected by the disease because these systems play a central role in resting brain activity as part of the default network” ([60] p. 29). Third, the large impact of AD on the DN might coherently explain large parts of cognitive symptoms in early AD. Impairments in “navigating in time, space and social affairs for distinct purposes” (see above) might contribute to well-known memory or spatial orientation deficits in AD but also to less apparent problems in planning and imagining future

events or in understanding sudden theme changes during talks with others.

ACKNOWLEDGEMENT

This work was supported by the German Federal Ministry of Education and Research Grant 01EV0710 and by Kommission für Klinische Forschung, Klinikum Rechts der Isar, München Grant 8765160.

We thank two reviewers and particularly Nick Meyers for constructive suggestions.

ABBREVIATIONS

AD	=	Alzheimer's disease
BOLD	=	Blood oxygenation level dependent
DN	=	Default network
FC	=	Functional connectivity
MTL	=	Medial temporal lobe
HC	=	Hippocampus
ICA	=	Independent component analysis
ROI	=	Region of interest
rs-fcMRI	=	Resting-state functional connectivity magnetic resonance imaging
RSN	=	Resting-state network
SBA	=	Spontaneous brain activity
SBF	=	Spontaneous BOLD fluctuation

CONFLICT OF INTEREST

There is no conflict of interest for any of the authors.

REFERENCES

- [1] Blennow K, de Leon MJ, Zetterberg H. Alzheimer's disease. *Lancet* 368: 387-403 (2006).
- [2] Sperling R. Functional MRI studies of associative encoding in normal aging, mild cognitive impairment, and Alzheimer's disease. *Ann NY Acad Sci* 1097: 146-155 (2007).
- [3] Dickerson BC, Salat DH, Bates JF, Atiya M, Killiany RJ, Greve DN, *et al.* Medial temporal lobe function and structure in mild cognitive impairment. *Ann Neurol* 56: 27-35 (2004).
- [4] Dickerson BC, Salat DH, Greve DN, Chua EF, Rand-Giovannetti E, Rentz DM, *et al.* Increased hippocampal activation in mild cognitive impairment compared to normal aging and AD. *Neurology* 65: 404-411 (2004).
- [5] Lustig C, Snyder AZ, Bhakta M, O'Brien KC, McAvoy M, Raichle ME, *et al.* Functional deactivations: change with age and dementia of the Alzheimer type. *Proc Natl Acad Sci USA* 100: 14504-14509 (2003).
- [6] Rombouts SA, Barkhof F, Goekoop R, Stam CJ, Scheltens P. Altered resting state networks in mild cognitive impairment and mild Alzheimer's disease: an fMRI study. *Hum Brain Mapp* 26: 231-239 (2005).
- [7] Buzsaki G, Draguhn A. Neuronal oscillations in cortical networks. *Science* 304: 1926-1929 (2004).
- [8] Llinas RR. The intrinsic electrophysiological properties of mammalian neurons: insights into central nervous system function. *Science* 242: 1654-1664 (1988).
- [9] Boly M, Balteau E, Schnakers C, Degueldre C, Moonen G, Luxen A, *et al.* Baseline brain activity fluctuations predict somatosensory perception in humans. *Proc Natl Acad Sci USA* 104: 12187-12192 (2007).

- [10] Fox MD, Snyder AZ, Vincent JL, Raichle ME. Intrinsic fluctuations within cortical systems account for intertrial variability in human behavior. *Neuron* 56: 171-184 (2007).
- [11] Fox MD, Snyder AZ, Zacks JM, Raichle ME. Coherent spontaneous activity accounts for trial-to-trial variability in human evoked brain responses. *Nat Neurosci* 9: 23-25 (2006).
- [12] Weissman DH, Roberts KC, Visscher KM, Woldorff MG. The neural bases of momentary lapses in attention. *Nat Neurosci* 9: 971-978 (2006).
- [13] Greicius MD, Srivastava G, Reiss AL, Menon V. Default-mode network activity distinguishes Alzheimer's disease from healthy aging: evidence from functional MRI. *Proc Natl Acad Sci USA* 101: 4637-4642 (2004).
- [14] Li SJ, Li Z, Wu G, Zhang MJ, Franczak M, Antuono PG. Alzheimer Disease: evaluation of a functional MR imaging index as a marker. *Radiology* 225: 253-259 (2002).
- [15] Sorg C, Riedl V, Muhlau M, Calhoun VD, Eichele T, Laer L, *et al.* Selective changes of resting-state networks in individuals at risk for Alzheimer's disease. *Proc Natl Acad Sci USA* 104: 18760-18765 (2007).
- [16] Supekar K, Menon V, Rubin D, Musen M, Greicius MD. Network analysis of intrinsic functional brain connectivity in Alzheimer's disease. *PLoS Comput Biol* 4: e1000100 (2008).
- [17] Fox MD, Raichle ME. Spontaneous fluctuations in brain activity observed with functional magnetic resonance imaging. *Nat Rev Neurosci* 8: 700-711 (2007).
- [18] Raichle ME, Mintun MA. Brain work and brain imaging. *Annu Rev Neurosci* 29: 449-476 (2006).
- [19] Matthews PM, Honey GD, Bullmore ET. Applications of fMRI in translational medicine and clinical practice. *Nat Rev Neurosci* 7: 732-744 (2006).
- [20] Biswal B, Yetkin FZ, Haughton VM, Hyde JS. Functional connectivity in the motor cortex of resting human brain using echo-planar MRI. *Magn Reson Med* 34: 537-541 (1995).
- [21] Beckmann CF, Smith SM. Tensorial extensions of independent component analysis for multisubject FMRI analysis. *Neuroimage* 25: 294-311 (2005).
- [22] Damoiseaux JS, Rombouts SA, Barkhof F, Scheltens P, Stam CJ, Smith SM, *et al.* Consistent resting-state networks across healthy subjects. *Proc Natl Acad Sci USA* 103: 13848-13853 (2006).
- [23] De Luca M, Beckmann CF, De Stefano N, Matthews PM, Smith SM. fMRI resting state networks define distinct modes of long-distance interactions in the human brain. *Neuroimage* 29: 1359-1367 (2006).
- [24] Hampson M, Peterson BS, Skudlarski P, Gatenby JC, Gore JC. Detection of functional connectivity using temporal correlations in MR images. *Hum Brain Mapp* 15: 247-262 (2002).
- [25] Buckner RL, Snyder AZ, Shannon BJ, LaRossa G, Sachs R, Fotenos AF, *et al.* Molecular, structural, and functional characterization of Alzheimer's disease: evidence for a relationship between default activity, amyloid, and memory. *J Neurosci* 25: 7709-7717 (2005).
- [26] Buckner RL, Vincent JL. Unrest at rest: Default activity and spontaneous network correlations. *Neuroimage* 37: 1091-1096; discussion 1097-9 (2007).
- [27] Greicius M. Resting-state functional connectivity in neuropsychiatric disorders. *Curr Opin Neurol* 21: 424-430 (2008).
- [28] He BJ, Shulman GL, Snyder AZ, Corbetta M. The role of impaired neuronal communication in neurological disorders. *Curr Opin Neurol* 20: 655-660 (2007).
- [29] Seeley WW, Crawford RK, Zhou J, Miller BL, Greicius MD. Neurodegenerative diseases target large-scale human brain networks. *Neuron* 62: 42-52 (2009).
- [30] Ogawa S, Lee TM, Kay AR, Tank DW. Brain Magnetic Resonance Imaging with Contrast Dependent on Blood Oxygenation. *Proc Natl Acad Sci USA* 87: 9868-9872 (1990).
- [31] Buxton RB, Uludag K, Dubowitz DJ, Liu TT. Modeling the hemodynamic response to brain activation. *Neuroimage* 23 (Suppl 1): S220-33 (2004).
- [32] Fox PT, Raichle ME. Focal physiological uncoupling of cerebral blood flow and oxidative metabolism during somatosensory stimulation in human subjects. *Proc Natl Acad Sci USA* 83: 1140-1144 (1986).
- [33] Logothetis NK, Pauls J, Augath M, Trinath T, Oeltermann A. Neurophysiological investigation of the basis of the fMRI signal. *Nature* 412: 150-157 (2001).
- [34] Logothetis NK, Wandell BA. Interpreting the BOLD signal. *Annu Rev Physiol* 66: 735-769 (2004).
- [35] Viswanathan A, Freeman RD. Neurometabolic coupling in cerebral cortex reflects synaptic more than spiking activity. *Nat Neurosci* 10: 1308-1312 (2007).
- [36] Vincent JL, Patel GH, Fox MD, Snyder AZ, Baker JT, Van Essen DC, *et al.* Intrinsic functional architecture in the anaesthetized monkey brain. *Nature* 447: 83-86 (2007).
- [37] Hagmann P, Cammoun L, Gigandet X, Meuli R, Honey CJ, Wedeen VJ, *et al.* Mapping the structural core of human cerebral cortex. *PLoS Biol* 6: e159 (2008).
- [38] Shmuel A, Leopold DA. Neuronal correlates of spontaneous fluctuations in fMRI signals in monkey visual cortex: Implications for functional connectivity at rest. *Hum Brain Mapp* 29: 751-761 (2008).
- [39] Goldman RI, Stern JM, Engel J, Jr, Cohen MS. Simultaneous EEG and fMRI of the alpha rhythm. *Neuroreport* 13: 2487-2492 (2002).
- [40] Laufs H, Holt JL, Elfont R, Krams M, Paul JS, Krakow K, *et al.* Where the BOLD signal goes when alpha EEG leaves. *Neuroimage* 31: 1408-1418 (2006).
- [41] Moosmann M, Ritter P, Krastel I, Brink A, Thees S, Blankenburg F, *et al.* Correlates of alpha rhythm in functional magnetic resonance imaging and near infrared spectroscopy. *Neuroimage* 20: 145-158 (2003).
- [42] Mantini D, Perrucci MG, Del Gratta C, Romani GL, Corbetta M. Electrophysiological signatures of resting state networks in the human brain. *Proc Natl Acad Sci USA* 104: 13170-13175 (2007).
- [43] Hampson M, Driesen NR, Skudlarski P, Gore JC, Constable RT. Brain connectivity related to working memory performance. *J Neurosci* 26: 13338-13343 (2006).
- [44] Seeley WW, Menon V, Schatzberg AF, Keller J, Glover GH, Kenna H, *et al.* Dissociable intrinsic connectivity networks for salience processing and executive control. *J Neurosci* 27: 2349-2356 (2007).
- [45] Birn RM, Diamond JB, Smith MA, Bandettini PA. Separating respiratory-variation-related fluctuations from neuronal-activity-related fluctuations in fMRI. *Neuroimage* 31: 1536-1548 (2006).
- [46] Fox MD, Snyder AZ, Vincent JL, Corbetta M, Van Essen DC, Raichle ME. The human brain is intrinsically organized into dynamic, anticorrelated functional networks. *Proc Natl Acad Sci USA* 102: 9673-9678 (2005).
- [47] Fransson P. Spontaneous low-frequency BOLD signal fluctuations: an fMRI investigation of the resting-state default mode of brain function hypothesis. *Hum Brain Mapp* 26: 15-29 (2005).
- [48] Vincent JL, Snyder AZ, Fox MD, Shannon BJ, Andrews JR, Raichle ME, *et al.* Coherent spontaneous activity identifies a hippocampal-parietal memory network. *J Neurophysiol* 96: 3517-3531 (2006).
- [49] Achard S, Salvador R, Whitcher B, Suckling J, Bullmore E. A resilient, low-frequency, small-world human brain functional network with highly connected association cortical hubs. *J Neurosci* 26: 63-72 (2006).
- [50] Calhoun VD, Adali T, Pearlson GD, Pekar JJ. A method for making group inferences from functional MRI data using independent component analysis. *Hum Brain Mapp* 14: 140-151 (2001).
- [51] Beckmann CF, Smith SM. Probabilistic independent component analysis for functional magnetic resonance imaging. *IEEE Trans Med Imaging* 23: 137-152 (2004).
- [52] Calhoun VD, Adali T, Giuliani NR, Pekar JJ, Kiehl KA, Pearlson GD. Method for multimodal analysis of independent source differences in schizophrenia: Combining gray matter structural and auditory oddball functional data. *Hum Brain Mapping* 27: 47-62 (2006).
- [53] Allen G, Barnard H, McColl R, Hester AL, Fields JA, Weiner MF, *et al.* Reduced hippocampal functional connectivity in Alzheimer disease. *Arch Neurol* 64: 1482-1487 (2007).
- [54] Wang L, Zang Y, He Y, Liang M, Zhang X, Tian L, *et al.* Changes in hippocampal connectivity in the early stages of Alzheimer's disease: evidence from resting state fMRI. *Neuroimage* 31: 496-504 (2006).
- [55] Braak H, Braak E. Neuropathological staging of Alzheimer-related changes. *Acta Neuropathol (Berl)* 82: 239-259 (1991).
- [56] Jack CR, Jr. Structural imaging approaches to Alzheimer's disease. In: Scinto LFM, Daffner KR (Eds.). *Early diagnosis and treatment of Alzheimer's disease*. Totowa: Human Press 2000; pp. 127-148.

- [57] Kahn I, Andrews-Hanna JR, Vincent JL, Snyder AZ, Buckner RL. Distinct cortical anatomy linked to subregions of the medial temporal lobe revealed by intrinsic functional connectivity. *J Neurophysiol* 100: 127-139 (2008).
- [58] Raichle ME, MacLeod AM, Snyder AZ, Powers WJ, Gusnard DA, Shulman GL. A default mode of brain function. *Proc Natl Acad Sci USA* 98: 676-682 (2001).
- [59] Wang K, Liang M, Wang L, Tian L, Zhang X, Li K, *et al.* Altered functional connectivity in early Alzheimer's disease: A resting-state fMRI study. *Hum Brain Mapp* 28: 967-978 (2007).
- [60] Buckner RL, Andrews-Hanna JR, Schacter DL. The brain's default network: anatomy, function, and relevance to disease. *Ann NY Acad Sci* 1124: 1-38 (2008).
- [61] Greicius MD, Krasnow B, Reiss AL, Menon V. Functional connectivity in the resting brain: a network analysis of the default mode hypothesis. *Proc Natl Acad Sci USA* 100: 253-258 (2003).
- [62] Mason MF, Norton MI, Van Horn JD, Wegner DM, Grafton ST, Macrae CN. Wandering minds: the default network and stimulus-independent thought. *Science* 315: 393-395 (2007).
- [63] McKiernan KA, D'Angelo BR, Kaufman JN, Binder JR. Interrupting the "stream of consciousness": an fMRI investigation. *Neuroimage* 29: 1185-1191 (2006).
- [64] Buckner RL, Carroll DC. Self-projection and the brain. *Trends Cogn Sci* 11: 49-57 (2007).
- [65] Gusnard DA, Raichle ME, Raichle ME. Searching for a baseline: functional imaging and the resting human brain. *Nat Rev Neurosci* 2: 685-694 (2001).
- [66] Celone KA, Calhoun VD, Dickerson BC, Atri A, Chua EF, Miller SL, *et al.* Alterations in memory networks in mild cognitive impairment and Alzheimer's disease: an independent component analysis. *J Neurosci* 26: 10222-10231 (2006).
- [67] Kahn I, Andrews-Hanna JR, Vincent JL, Snyder AZ, Buckner RL. Distinct cortical anatomy linked to subregions of the medial temporal lobe revealed by intrinsic functional connectivity. *J Neurophysiol* 100: 129-139 (2008).
- [68] Baliki MN, Chialvo DR, Geha PY, Levy RM, Harden RN, Parrish TB, *et al.* Chronic pain and the emotional brain: specific brain activity associated with spontaneous fluctuations of intensity of chronic back pain. *J Neurosci* 26: 12165-12173 (2006).
- [69] Fox MD, Zhang D, Snyder AZ, Raichle ME. The global signal and observed anticorrelated resting state brain networks. *J Neurophysiol* 101: 3270-3283 (2009).
- [70] Fox MD, Zhang D, Snyder AZ, Raichle ME. The global signal and observed anticorrelated resting state brain networks. *J Neurophysiol* 101: 3270-3283 (2009).
- [71] Murphy K, Birn RM, Handwerker DA, Jones TB, Bandettini PA. The impact of global signal regression on resting state correlations: are anti-correlated networks introduced? *Neuroimage* 44: 893-905 (2009).
- [72] Petrella JR, Wang L, Krishnan S, Slavin MJ, Prince SE, Tran TT, *et al.* Cortical deactivation in mild cognitive impairment: high-field-strength functional MR imaging. *Radiology* 245: 224-235 (2007).
- [73] Petrella JR, Prince SE, Wang L, Hellegers C, Doraiswamy PM. Prognostic value of posteromedial cortex deactivation in mild cognitive impairment. *PLoS ONE* 2: e1104 (2007).
- [74] Bassett DS, Bullmore E. Small-world brain networks. *Neuroscientist* 12: 512-523 (2006).
- [75] Watts DJ, Strogatz SH. Collective dynamics of 'small-world' networks. *Nature* 393: 440-442 (1998).
- [76] Latora V, Marchiori M. Efficient behavior of small-world networks. *Phys Rev Lett* 87: 198701 (2001).
- [77] Bullmore E, Fadili J, Breakspear M, Salvador R, Suckling J, Brammer M. Wavelets and statistical analysis of functional magnetic resonance images of the human brain. *Stat Methods Med Res* 12: 375-399 (2003).
- [78] Bullmore E, Fadili J, Maxim V, Sendur L, Whitcher B, Suckling J, *et al.* Wavelets and functional magnetic resonance imaging of the human brain. *Neuroimage* 23 (Suppl 1): S234-49 (2004).
- [79] Sporns O, Zwi JD. The small world of the cerebral cortex. *Neuroinformatics* 2: 145-162 (2004).
- [80] He Y, Chen Z, Evans A. Structural insights into aberrant topological patterns of large-scale cortical networks in Alzheimer's disease. *J Neurosci* 28: 4756-4766 (2008).
- [81] Stam CJ, Jones BF, Nolte G, Breakspear M, Scheltens P. Small-world networks and functional connectivity in Alzheimer's disease. *Cereb Cortex* 17: 92-99 (2007).
- [82] Riedl V, Honey CJ. Alzheimer's disease: a search for broken links. *J Neurosci* 28: 8148-8149 (2008).
- [83] Deshpande G, Laconte S, Peltier S, Hu X. Integrated local correlation: A new measure of local coherence in fMRI data. *Hum Brain Mapp* 30(1): 13-23 (2009).
- [84] Kriegeskorte N, Goebel R, Bandettini P. Information-based functional brain mapping. *Proc Natl Acad Sci USA* 103: 3863-3868 (2006).
- [85] Zang Y, Jiang T, Lu Y, He Y, Tian L. Regional homogeneity approach to fMRI data analysis. *Neuroimage* 22: 394-400 (2004).
- [86] Xu Y, Xu G, Wu G, Antuono P, Rowe DB, Li SJ. The phase shift index for marking functional asynchrony in Alzheimer's disease patients using fMRI. *Magn Reson Imaging* 26: 379-392 (2008).
- [87] He Y, Wang L, Zang Y, Tian L, Zhang X, Li K, *et al.* Regional coherence changes in the early stages of Alzheimer's disease: a combined structural and resting-state functional MRI study. *Neuroimage* 35: 488-500 (2007).
- [88] Bai F, Zhang Z, Yu H, Shi Y, Yuan Y, Zhu W, *et al.* Default-mode network activity distinguishes amnesic type mild cognitive impairment from healthy aging: a combined structural and resting-state functional MRI study. *Neurosci Lett* 438: 111-115 (2008).
- [89] Arendt T. Synaptic plasticity and cell cycle activation in neurons are alternative effector pathways: the 'Dr. Jekyll and Mr. Hyde concept' of Alzheimer's disease or the yin and yang of neuroplasticity. *Prog Neurobiol* 71: 83-248 (2003).
- [90] Hyman BT, Van Hoesen GW, Damasio AR. Memory-related neural systems in Alzheimer's disease: an anatomic study. *Neurology* 40: 1721-1730 (1990).
- [91] Mesulam MM. A plasticity-based theory of the pathogenesis of Alzheimer's disease. *Ann N Y Acad Sci* 924: 42-52 (2000).